ISSN 1063-7761, Journal of Experimental and Theoretical Physics, 2020, Vol. 130, No. 4, pp. 571–578. © Pleiades Publishing, Inc., 2020.
Russian Text © The Author(s), 2020, published in Zhurnal Eksperimental'noi i Teoreticheskoi Fiziki, 2020, Vol. 157, No. 4, pp. 679–687.

ORDER, DISORDER, AND PHASE TRANSITION IN CONDENSED SYSTEM

High-Precision Studies of the Compressibility and Relaxation of g-As_2S_3 Glasses at High Hydrostatic Pressures up to 8.6 GPa

V. V. Brazhkin[a,*], E. Bychkov[b], A. S. Tver'yanovich[c], and O. B. Tsiok[a,]**

[a] *Vereshchagin Institute of High-Pressure Physics, Troitsk, Moscow, 108840 Russia*
[b] *LPCA, UMR 8101 CNRS, Universite du Littoral, Dunkerque, 59140 France*
[c] *Institute of Chemistry, St. Petersburg State University, St. Petersburg, 198504 Russia*
**e-mail: brazhkin@hppi.troitsk.ru*
***e-mail: tsiok@hppi.troitsk.ru*

Received October 23, 2019; revised October 23, 2019; accepted November 5, 2019

Abstract—The high-precision volume measurements of the g-As_2S_3 glass have been performed at high hydrostatic pressures up to 8.6 GPa, and room temperature. The glass behaves elastically during compression only at pressures up to 1.5 GPa; at higher pressures, a smooth transformation and inelastic density relaxation (logarithmic in time) take place. In the initial segment, the bulk modulus is $B = 13.5 \pm 0.15$ GPa and its pressure derivative is $dB/dP = 6.2 \pm 0.2$. When pressure increases further, the relaxation rate passes through a maximum at 4 GPa, which is accompanied by a bulk modulus plateau, and then decreases and remains noticeable up to the maximum pressure. When pressure decreases, inelastic behavior and the reverse transformation are observed at pressures below 4 GPa. After pressure release, the g-As_2S_3 glasses have a residual densification of about 3% and their optical properties differ substantially from the initial ones. The glass density relaxes to a quasi-equilibrium value in several months under normal conditions. The kinetics of the Raman spectrum and the optical absorption edge of the glasses during relaxation is studied under normal pressure. The data on compressibility of glasses and comparative Raman studies of initial and compacted glasses show that at pressures up to 9 GPa, there is a strong increase in chemical disorder in the glass, while there is no significant change in the coordination number.

DOI: 10.1134/S1063776120030024

INTRODUCTION

g-As_2S_3-based glasses have received the most study and are most widely used among the chalcogenide materials. Glass formation in cooling the As_2S_3 melt was described for the first time in 1870 [1], and the properties of the glass were comprehensively studied in [2]. As_2S_3-based glasses are widely used due to their high transparency in the middle IR region, anomalous photoelastic properties, and so on [3, 4]. Sulfide and selenide As_2S_3 sesquichalcogenides have a layered structure, where two-dimensional layers are formed by As_6X_6 rings and each arsenic atom belongs to three neighboring rings. A similar two-dimensional structure is retained in glass; however, a single type of rings in crystals changes into a broad distribution [5].

The short-range and intermediate orders of crystalline As_2S_3 (orpiment) are substantially retained in the liquid and glassy states; hence, their electronic structures are similar [6, 7]. However, in contrast to the crystal, the atomic layers in the glass bend strongly, join each other, and form a continuous network. Note that it was g-As_2S_3 glass that served as a prototype for the famous Zachariasen model for a glass network [8]. The chemical disorder in g-As_2S_3 (ratio of the number of homopolar bonds to the total number of bonds) does not exceed 3–5%, which is well below that in g-As_2Se_3 and g-As_2Te_3 [3, 9].

The behavior of As_2S_3 during compression in the crystalline, glassy, and liquid states was studied in a few works. The unique close packing of layers in the crystal structure of orpiment leads to a high stability of this modification in compression: no phase transformations were detected at room temperature up to 10 GPa. However, the interlayer interaction increases strongly on compression and the optical gap decreases from 2.7 to 1.6 eV upon compression up to 10 GPa [10].

The authors of [11] predicted that a phase transition should occur in both crystalline and glassy As_2S_3, which is accompanied by metallization, at a pressure above 35–40 GPa. In [12], we found that the crystalline modification of As_2S_3 decomposes into a mixture of modifications with "wrong" stoichiometries AsS_2 and AsS at high temperatures (above 800 K) and pressures above 6 GPa. The room-temperature studies [13] of orpiment As_2S_3 at ultrahigh pressures up to 46 GPa

point to the absence of phase transformations over the entire pressure range: only weak structural distortion at 25 GPa and smooth metallization at 42 GPa can occur.

The behavior of g-As_2S_3 glass under pressure was investigated in many works (see [6, 11, 14–18]). The optical gap in g-As_2S_3 glass behaves similarly to the crystal: it decreases from 2.5 to 1.5 eV during compression to 8.6 GPa [15]. The ultrasonic investigations [11] of the elastic moduli of g-As_2S_3 were performed at pressures up to 2 GPa: the initial bulk compression modulus of g-As_2S_3 was found to be $B_0 = 12.84$ GPa, and the pr derivative of the modulus was $B_P' = 7.5$. Note that the data on Young's modulus and the shear modulus obtained in [2] give a higher bulk compression modulus ($B_0 = 13.7$ GPa). The Raman studies of g-As_2S_3 glass to a pressure of 10 GPa [18] indicate nanoseparation (enhanced chemical disorder in the glass). Apart from the fundamental excitation bands related to the vibrations of pyramidal AsS_3 groups, vibrational bands, which can be attributed to As_4S_4 groups, appear. Small irreversible changes in Raman spectra were retained after pressure release. The detailed investigation of IR spectra to a pressure of 57 GPa [6] found that the optical gap closed and metallic conduction appeared at about 45 GPa. Later [16], g-As_2S_3 was studied by EXAFS up to a pressure of 60 GPa. An anomalous increase in the As–S interparticle distance was detected over a wide pressure range from 15 to 50 GPa. This increase is obviously related to an increase in the coordination number. The denser modification of the glass at a pressure above 50 GPa is likely to be a metal. Finally, the short- and intermediate-range orders in the g-As_2S_3 glass at a pressure up to 6.5 GPa were investigated by ab initio computer simulation [17]. An increase in the number of dangling bonds and the number of "wrong" As–As neighbors was detected.

The As_2S_3 melt was studied under pressure in [19, 20]. The viscosity of the melt was found to decrease by four orders of magnitude (which is a record) along the melting curve during compression up to 8 GPa. At pressures above 6 GPa, the coordination number increases noticeably and the melt transforms into a semimetallic state. The melt was assumed to undergo nanoseparation with the formation of regions with wrong stoichiometries AsS and AsS_2 on the scale of two coordination shells at these pressures. The same separation into a mixture of two modifications but on a macroscale was observed during solidification of the melt at $P > 6$ GPa [12].

Recently, we have performed a cycle of works to study the compressibility and relaxation of glassy selenium [21, 22], germanium-based chalcogenide glasses [23, 24], and glassy arsenic telluride (metallization of which was investigated in detail) [9, 25] and revealed a number of bright and unusual effects.

The purpose of this work is to study the compressibility and relaxation (during compression and after pressure release under normal conditions) of the g-As_2S_3 chalcogenide "archetype" glass at a high accuracy.

EXPERIMENTAL

The initial glasses were made of elementary As (99.9999%) and S (99.999%, Aldrich Chemical Ltd.). The substances were placed in preliminarily cleaned quartz tubes with an inside diameter of 8 mm, which were then pumped out and sealed. The melts were held and stirred at 600°C for 6 h and were then water cooled.

Comparative structural and Raman studies were carried out for the following two groups of glasses under normal conditions: the quenched glasses are the initial glasses after melt quenching, and the glasses after high pressure are the samples subjected to a pressure of 8.6 GPa.

Raman spectra were measured on a spectrometer equipped with a Sentera (Bruker) microscope during excitation by a solid-state laser with a wavelength of 785 nm. Although the laser wavelength corresponds to the transparent region of the sample, the laser power was decreased to 1 mW during measurements. Absorption spectra were measured on a UV-3600 (Shimadzu) spectrophotometer. The refractive index was determined from the defocusing of an image when a sample was placed between the image and the microscope objective lens using the expression $n = (1 - t/d)^{-1}$, where d is the plane-parallel sample plate thickness and t is the change in the focal distance. The measurements were performed with an MIK-1 IR microscope at a wavelength of 1.2 μm.

The initial melt-quenched glass samples had a density of 3.18 g/cm^3. During preparation for high-pressure experiments (cementing of strain gauges followed by "hot" cement polymerization at $T = 155$°C for 7 h), the glass samples relaxed to a more equilibrium state, internal stresses were removed, and the density increased to 3.19 g/cm^3. All glass samples (initial samples and samples after high-pressure experiments) had a typical glass structure and did not contain crystalline impurities (see Fig. 1). The samples intended for high-pressure experiments were parallelepipeds with smoothed edges. Samples $3 \times 2 \times 1.7$ mm^3 in size were used for compressibility and relaxation investigations (see Fig. 2).

High-pressure experiments were carried out in a Toroid apparatus [26] with the central pip diameter of 15 mm. The tensometric technique [27] was used to measure the glassy sample volume under hydrostatic pressure (see Fig. 3). The absolute accuracy of measuring the sample volume using this technique was 0.2% and the measurement sensitivity was 10^{-3}%. An important advantage of this technique is a very short

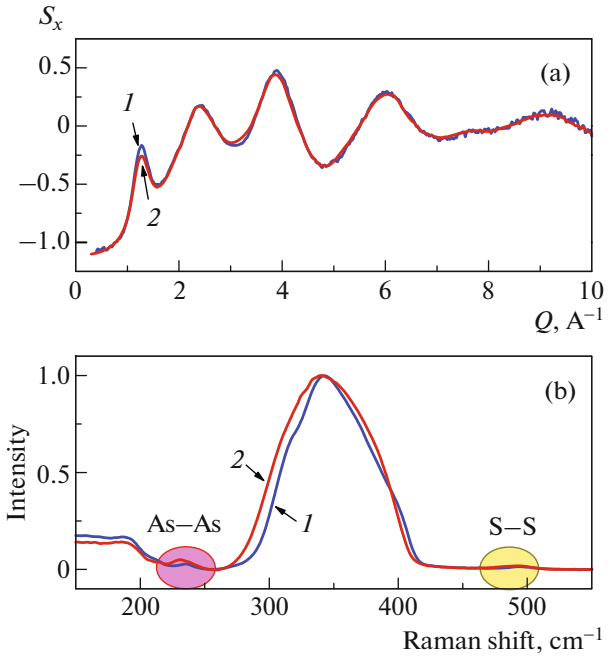

Fig. 1. (Color online) (a) Structure factors and (b) Raman spectra of g-As_2S_3 samples (*1*) before and (*2*) after the action of a high pressure.

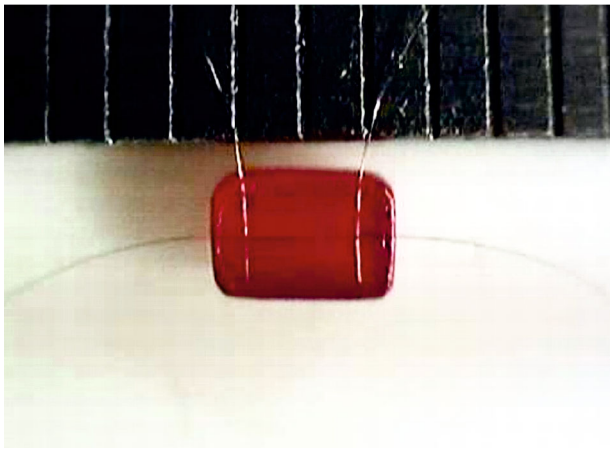

Fig. 2. (Color online) g-As_2S_3 glass sample with a glued strain gage.

Fig. 3. (Color online) Sample (for calibration) and the manganin gage in an ampule with a hydrostatic medium.

measurement time (0.2 s). As a result, detailed information on the behavior of the sample volume under pressure can be obtained. Moreover, this technique makes it possible to study the volume change kinetics under pressure over a wide time range (10–10^7 s). An important advantage of this technique is the fact that baric dependences of the sample volume can be obtained when pressure increases or decreases under purely hydrostatic conditions. This technique was successfully applied to investigate both oxide and chalcogenide glasses (see, e.g. [9, 21–25, 28, 29]).

A methanol–ethanol (4 : 1) mixture with a hydrostatic limit of about 10 GPa was used as a pressure-transferring medium. The pressure was measured by a manganin transducer calibrated against the transitions in bismuth (2.54 and 7.7 GPa). The reproducibility of the pressure scale (possibility of comparison of the data obtained in different experiments at the same pressure) was 3 MPa in all experiments.

The sample volume was measured when the pressure was continuously changed at a rate of 0.07–0.12 GPa/min upon increasing and 0.03–0.05 GPa/min upon decreasing. To plot baric dependences, we took data at a pressure step of 0.025 GPa, which allowed us to plot an almost continuous curve without extrapolation.

The pressure was maintained at a constant level accurate to ±2 MPa during measurements when the glass densification kinetics was studied at a fixed pressure. Both the tensometric technique and the measurement of Raman spectra were used to investigate the relaxation kinetics at normal pressure.

RESULTS AND DISCUSSION

Figure 4 shows the baric dependences of the g-As_2S_3 glass volume for three different samples.

The compression curve of the g-As_2S_3 glasses cannot be approximated by a simple equation of state, and elastic behavior is only observed to a pressure of 1.3–1.5 GPa. As compared to other chalcogenide glasses, the pressure hysteresis between the compression and unloading curves is small, the residual densification is about 3%, and the volume relaxes to the initial value in several months under normal conditions. The inset to Fig. 4 shows the segments of the baric dependences of the glass volume near 6–7 GPa to demonstrate the measurement accuracy. Relaxation measurements were carried out on one of the samples at several fixed

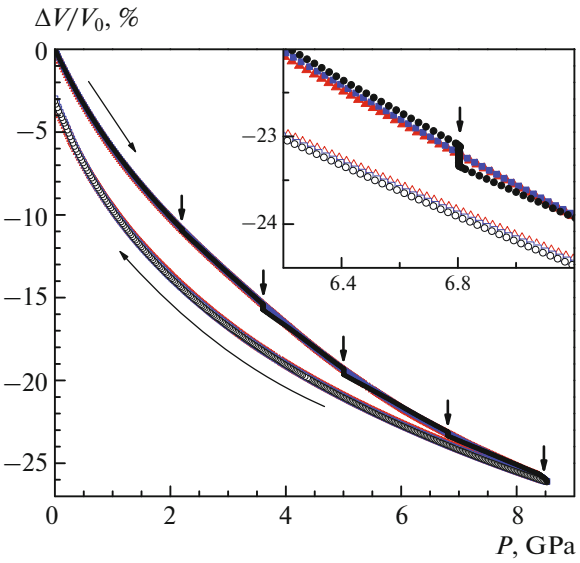

Fig. 4. (Color online) Compressibility of the As_2S_3 glass during an increase (solid symbols) and decrease (open symbols) of the pressure. (The colors and symbols indicating different experiments are the same in all figures.) The glass densification kinetics at a fixed pressure was studied in one of the experiments at a fixed pressure and the points indicated by arrows. The holding time at the maximum pressure in that experiment was about 20 h, and the holding time in two other experiments was less than 1 h. (inset) Enlarged high-pressure region.

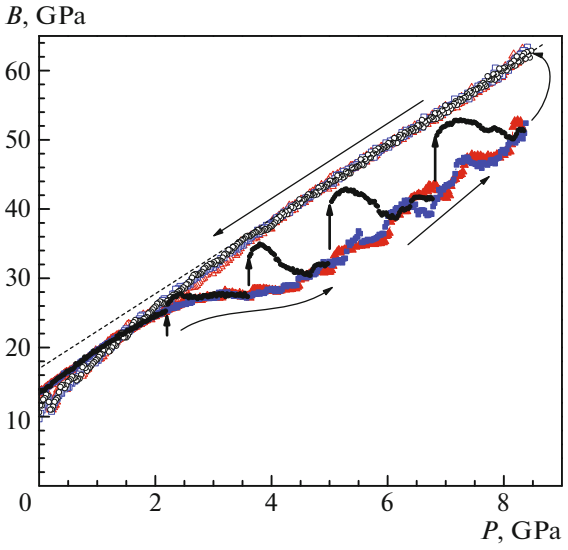

Fig. 5. (Color online) Effective bulk moduli of the g-As_2S_3 glass obtained from the initial $V(P)$ data as $B = -VdP/dV$ during an increase (solid symbols) and decrease (open symbols) of the pressure. The heavy arrows indicate holding at a constant pressure (see Fig. 4). The dashed line illustrates the nonlinearity of the pressure dependence of the bulk modulus when pressure decreases.

pressures. The baric dependences of three samples are seen to coincide at a high accuracy (about 0.1%), and the compression curve recorded after isobaric relaxation in the course of a further increase in the pressure merges asymptotically with the compression curve for which relaxation measurements were not performed.

Due to the high sensitivity of the tensometric technique, we were able to find the effective bulk compression moduli of the glasses by direct differentiation at points without additional processing. Figure 5 shows the bulk compression moduli of the g-As_2S_3 glasses versus pressure. A linear increase in the bulk compression modulus with pressure is observed up to 1.2 GPa. In the initial segment, the bulk modulus is $B = 13.5 \pm 0.15$ GPa and its pressure derivative is $dB/dP = 6.2 \pm 0.2$. This value is noticeably higher than that determined in the ultrasonic measurements (12.9 GPa) [11] and is slightly lower than the estimate made from Young's modulus (13.7 GPa) [2]. The bulk compression modulus of the g-As_2S_3 glasses obeys the general dependence obtained for analog glasses: $B = 14.5$ GPa for g-As_2Se_3 [14] and $B = 15.8$ GPa for g-As_2Te_3 [25]. When the pressure increases further, the dB/dP derivative decreases and becomes almost zero in the range 2.5–4 GPa. The decrease in the effective bulk compression modulus of the g-As_2S_3 glasses in the pressure range 2.5–4 GPa is substantially analogous to the behavior of the g-$GeSe_2$ and g-As_2Te_3 glasses [9, 23–25]. This behavior of the modulus is caused by intense volume relaxation, which begins above 1.5 GPa and continues up to the highest pressures. The bulk modulus in this range corresponds to the relaxing values. The difference between the relaxing and fully relaxed bulk moduli indicates the presence of activation processes and diffuse transitions in the glasses (see discussion in [29]). Upon long-term isobaric relaxation, the effective bulk modulus first corresponds to high relaxed values when the pressure increases and then decreases to the effective relaxing values, which correspond to the curve recorded at a constant loading rate (modulus "forgets" the history; see Fig. 5). The small irregularities in the relaxing modulus reproduce the variation in the rate of change of pressure in the range where relaxation takes place.

On pressure release, the glasses behave elastically down to 4 GPa and the bulk modulus corresponds to the relaxed values. The baric derivative of the relaxed bulk modulus is $dB/dP = 5.4$ when pressure decreases. The bulk moduli of the g-As_2S_3 glasses during pressure release are close to the corresponding moduli after isobaric relaxation when pressure increases (see Fig. 5), which points to the same short-range structure of these glasses when pressure increases or decreases. At lower pressures, the effective bulk modulus decreases more rapidly, which is associated with relaxation during the reverse transformation, and this transformation is not completed down to atmospheric pressure.

At pressures above 2 GPa, a noticeable time dependence of the g-As_2S_3 glass volume takes place at a fixed

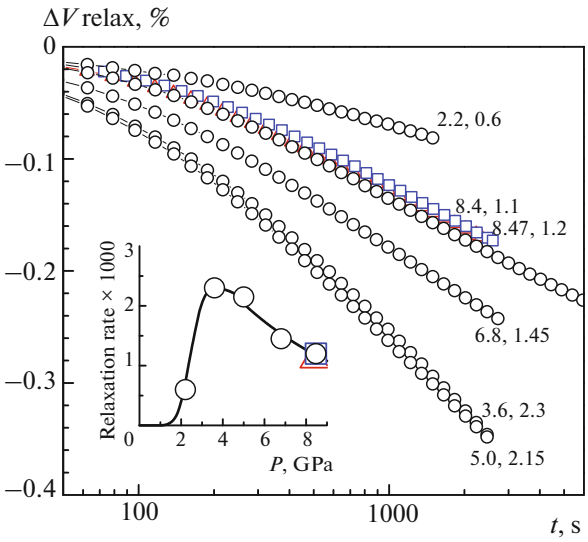

Fig. 6. (Color online) Relaxation of the As_2S_3 glass volume at a fixed pressure. The digits at the curves correspond to the exposure pressure in GPa and to the slope of the linear part of the curves. During holding at the maximum pressure, the pressure drifted slowly, and the relaxation dependences were obtained by projecting the experimental $V(P, t)$ data onto vertical P = const along the relaxed dV/dP slope. The pressure was maintained accurate to 20–30 bar on holding at intermediate pressures. (inset) Pressure dependence of the steady relaxation rate determined as $-d(V/V_0)/d(\log t)$ in the linear segment of the time dependences.

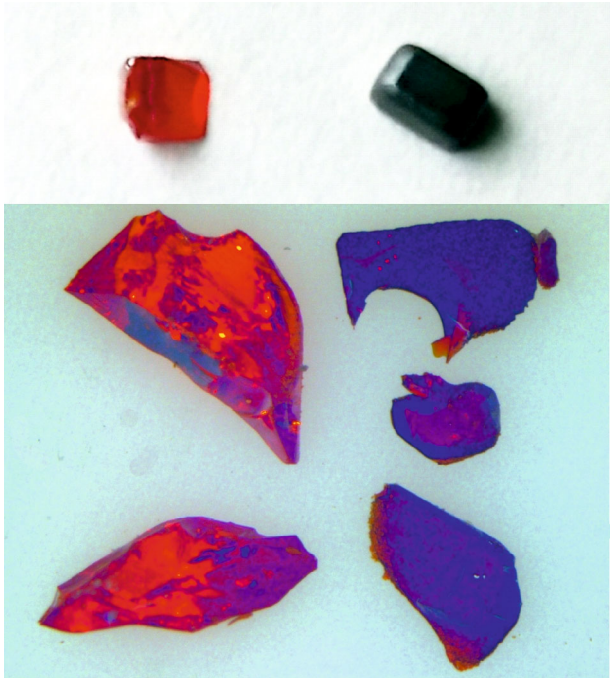

Fig. 7. (Color online) Initial (on the left) and pressure-treated (on the right) g-As_2S_3 glass samples. Large workpieces several millimeters in size are at the top, and small fragments 0.1–0.3 mm in size are at the bottom.

pressure (relaxation), and the change in the volume at long times is proportional to the logarithm of time (Fig. 6). The deviation from the logarithmic dependence at the initial segment is related to a finite rate of increase of pressure in the experiment: the processes with a relaxation time shorter than 100–300 s are partly or completely completed when pressure increases before holding. The relaxation rate is maximal at 3.5–4.5 GPa (see inset to Fig. 6). The absolute values of the maximum relaxation intensity are close to the corresponding maximum values of the g-As_2Te_3 glasses and the g-$GeSe_2$ glasses, where the type of connection of structural tetrahedra changes from edge-sharing to corner-sharing tetrahedra and the network is easily compressed in a narrow pressure range [23, 24]. The intense relaxation processes that occur in the g-As_2S_3 glasses at a pressure of 3.5–4.5 GPa are likely to be related to the change in the type of connection of pyramids from edge-sharing to corner-sharing pyramids and to a simultaneous increase in the number of "wrong" neighbors. Similarly to the g-As_2Te_3 glasses, the relaxation processes in the g-As_2S_3 glasses and the decrease in the effective bulk modulus begin almost simultaneously at pressures above 1.5 GPa.

After pressure release, the g-As_2S_3 glasses have a residual densification of 3% and their optical properties differ substantially from the initial ones (see Fig. 7 and the text below).

Long-term holding at normal pressure is accompanied by logarithmic volume relaxation and the recovery of the density (see Fig. 8). It is interesting that logarithmic density relaxation is observed over a wide time range with a possible tendency toward saturation at times longer than 10^7 s.

As is seen in Fig. 7, the sample after pressure release is characterized by significant darkening, i.e., a shift of the fundamental absorption edge toward the IR region. This shift is about 100 nm (about 0.34 eV), as follows from the absorption spectra presented in Fig. 9.

The shift of the absorption edge is accompanied by a change in the short-range structure of the glass. Figure 10 shows the Raman spectra of the initial glass sample before pressure and after pressure release (for correct comparison of the spectra, we subtracted the baseline and performed normalization by the main peak at 340 cm^{-1}). The numbering of the curves corresponds to the numbering in Fig. 9.

As compared to the initial sample, the glass after pressure release has a wide main peak at 340 cm^{-1}, which is mainly caused by the totally symmetrical vibrations of the pyramidal structure of the As–$S_{3/2}$ structural unit [30] and a high intensity in the region of vibrations of the nonstoichiometric bonds As–As (235 cm^{-1} [31]) and S–S (490 cm^{-1} [31]). The high content of the homopolar bonds in the sample after

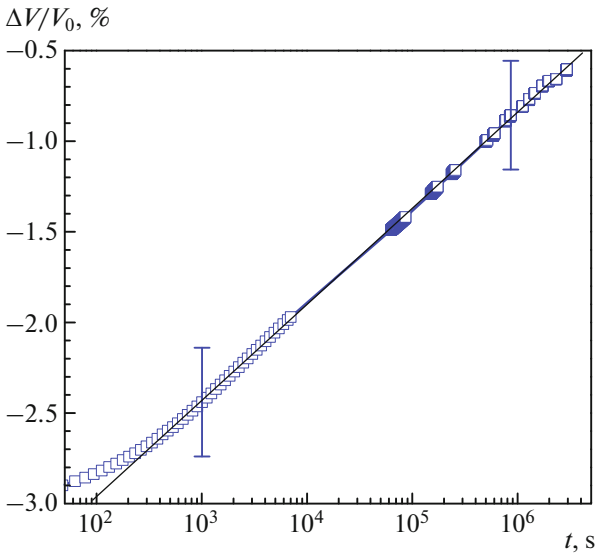

Fig. 8. (Color online) Relaxation of the g-As_2S_3 glass sample volume after pressure release. Error for two selected points 0.3% error bar corresponds to the possible systematic measurement error.

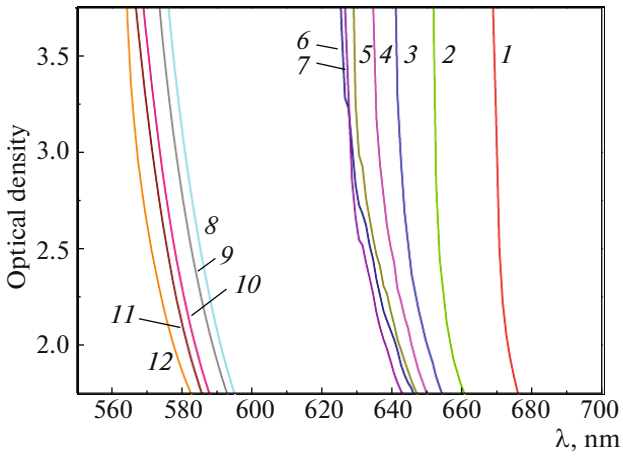

Fig. 9. (Color online) Absorption spectra of g-As_2S_3: (*1*) after pressure release; (*2–7*) room-temperature storage for 3, 7, 14, 25, 35, and 63 days, respectively, after pressure release; (*8–11*) room-temperature storage for 103 days followed by holding at $T = 140$°C for 1, 2, 5, and 10 h, respectively; and (*12*) initial sample.

pressure points to the disproportionation of the As_2S_3 compound in the glassy state at a pressure of 8.6 GPa. The disproportionation is facilitated by the closeness of the heteropolar bond energy and the averaged homopolar bond energy. The As–As and S–S bond energies are 146 and 226 kJ/mol, respectively [32]; therefore, the energy of the averaged homopolar bond is 186 kJ/mol. The As–S bond energy is estimated by the Pauling relation [33]

$$E_{A-B} = (E_{A-A}E_{B-B})^{1/2} + 96(X_A - X_B)^2,$$

where E is the bond energy and X is the electronegativity of atoms (2.18 for As and 2.58 for S). Thus, for the As–S bond, we obtain 197 kJ/mol, which is close to the averaged homopolar bond energy given above.

The storage of a sample at room temperature after pressure release leads to a gradual shift in the fundamental absorption edge toward the short-wavelength region of the spectrum. This relaxation process ends in a month (see Fig. 9), and the Raman spectrum does not undergo significant changes (see Fig. 10). When considering the fundamental absorption edge as a relaxing property, we have [34]

$$(y(t) - y(\infty))/(y(0) - y(\infty)) = \exp(-(t/\tau)^{\beta}),$$

where $y(0)$, $y(t)$, and $y(\infty)$ are the fundamental absorption edges at the initial time (sample after pressure release), at time t, and when relaxation reaches saturation (storage at room temperature for 63 days), respectively; τ is the relaxation time; and β is the Kohlrausch factor, which takes into account the existence of a relaxation time spectrum ($0 \le \beta \le 1$). The calculated values are $\tau = 7$ days and $\beta = 0.76$. Thus, we have a slow process with a wide relaxation time distribution, which does not include the chemical nature of the glass.

As a result, we have glass with time-stable properties, and the optical properties differ substantially from those of the initial g-As_2S_3 (before pressure treatment). The absorption edge shifts toward the long-wavelength region of the spectrum by 60 nm, and the refractive index is 2.57 at a wavelength of 1.2 μm, which is much higher than that of the initial glass (2.33). The structure of the glass is characterized by a large number of nonstoichiometric bonds. All these

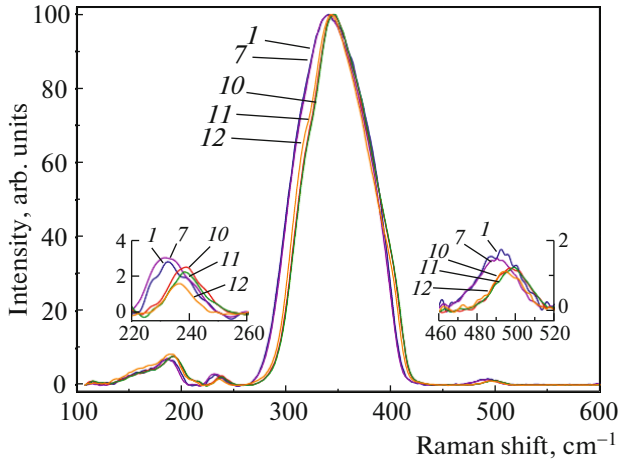

Fig. 10. (Color online) Raman spectra of g-As_2S_3: (*1*) after pressure release; (*7*) room-temperature storage for 63 days after pressure release; (*10*, *11*) room-temperature storage for 103 days followed by holding at $T = 140$°C for 5 and 10 h, respectively; and (*12*) initial sample. (inset) Enlarged spectral fragments at 235 and 490 cm^{-1}.

changes point to the photostructural transformations (maximum changes are $\Delta E = 0.1–0.3$ eV, $D_n = 0.1–0.3$) in chalcogenide glasses, mainly in g-As_2S_3. The light-induced darkening is removed by annealing at near-softening temperatures. For g-As_2S_3, T_g is 170–190°C [35]. To trace the recovery of the glass into the initial state, we chose the annealing temperature that corresponds to the beginning of structural relaxation upon heating of quenched g-As_2S_3, which was dilatometrically determined (140°C). The sample became much more transparent after annealing for 1 h (see Fig. 1). The refractive index decreased to 2.40 after annealing for 2 h. The excess intensity (as compared to initial sample) of the peak corresponding to the S–S bonds in Raman spectra disappeared, and the intensity of the peak corresponding to the As–As bonds decreased sharply after annealing for 5 h (Fig. 10).

Thus, the main relaxation and inelastic densification effects during compression of the g-As_2S_3 glass are related to the growth of the chemical disorder without increasing the coordination number. This conclusion supports the assumption about nanoseparation in the melt at high pressures [20] and agrees well with the data obtained for the decomposition of the supercritical modification at high pressures and temperatures ($As_2S_3 = AsS_2 + AsS$ [12]). The coordination number is thought to increase substantially at higher pressures (12–15 GPa), according to the EXAFS data [16]. Recall that the number of wrong bonds in the g-As_2Te_3 glasses, where the initial chemical disorder is very significant, decreases during compression [9, 25]. Therefore, the chemical disorder in the chalcogenide glasses at high pressures is determined by the compression-induced changes in their thermodynamic and kinetic parameters rather than by the ionicity.

Although photostructural transformations have recently been discovered, they are now widely used due to the possibility of controlling the transmission region and the refractive index of an IR optics material [36]. This finding is especially important because of the rapid development of fiber IR optics. Therefore, the effect revealed in this work has good practical application prospects.

CONCLUSIONS

The high-precision measurements of the g-As_2S_3 glass volume under hydrostatic pressure conditions allowed us to reveal the main features of the transition in the g-As_2S_3 glasses. The following pressure ranges were marked: up to 1.5 GPa, "normal" elastic behavior; from 1.5 to 3 GPa, beginning of inelastic behavior; from 3 to 5 GPa, polyamorphic transformation accompanied by an effective bulk modulus plateau and intense logarithmic density relaxation; and 5–8.6 GPa, inelastic behavior with moderate relaxation. The smooth transformation in these glasses is likely to be related to a strong increase in the chemical disorder and is only partly reversible. The optical properties of the initial glasses and the pressure-compacted glasses are strongly different, which is mainly associated with the chemical disorder. The effect detected in this work has prospects of practical application.

ACKNOWLEDGMENTS

We thank A.V. Gulyutin for his help in measuring the glass density.

FUNDING

This work was supported by the Russian Science Foundation, project no. 19-12-00111.

REFERENCES

1. C. Schultz-Sellack, Ann. Phys. Chem. **139**, 182 (1870).
2. F. V. Glaze et al., J. Res. Natl. Bureau Stand. **59**, 83 (1957).
3. A. Feltz, *Amorphe und Glasartige Anorganische Festktsrper* (Wiley-VCH, Akademie, Berlin, 1983).
4. O. Podrazky et al., Proc. SPIE **9450**, B1 (2015).
5. S. I. Simdyankin, S. R. Elliott, Z. Hajnal, T. A. Niehaus, and Th. Frauenheim, Phys. Rev. B **69**, 144202 (2004).
6. V. V. Struzhkin, A. F. Goncharov, R. Caracas, et al., Phys. Rev. B **77**, 165133 (2008).
7. O. Uemura, Y. Sagara, D. Muno, et al., J. Non-Cryst. Solids **30**, 155 (1978).
8. W. H. Zachariasen, J. Am. Chem. Soc. **54**, 3841 (1932).
9. V. V. Brazhkin, E. Bychkov, and O. B. Tsiok, Phys. Rev. B **95**, 054205 (2017).
10. R. Zallen, High Press. Res. **24**, 117 (2004).
11. D. Gerlich, E. Litov, and O. L. Andersen, Phys. Rev. B **20**, 2529 (1979).
12. N. B. Bolotina, V. V. Brazhkin, T. I. Dyuzheva, Y. Katayama, L. F. Kulikova, L. M. Lityagina, and N. A. Nikolaev, JETP Lett. **98**, 539 (2013).
13. K. Liu et al., Materials **12**, 784 (2019).
14. G. Parthasarathy and E. S. R. Gopal, Bull. Mater. Sci. **7**, 271 (1985).
15. B. A. Weinstein, R. Zallen, and M. L. Slade, J. Non-Cryst. Solids **35–36**, 1255 (1980).
16. M. Vaccari et al., J. Chem. Phys. **131**, 224502 (2009).
17. F. Shimojo, K. Hoshino, and Y. Zempo, J. Non-Cryst. Solids **312–314**, 388 (2002).
18. K. S. Andrikopoulos et al., J. Non-Cryst. Solids **352**, 4594 (2006).
19. V. V. Brazhkin, Y. Katayama, M. V. Kondrin, et al., Phys. Rev. Lett. **100**, 145701 (2008).
20. V. V. Brazhkin, Y. Katayama, M. V. Kondrin, et al., Phys. Rev. B **82**, 146202 (2010).
21. V. V. Brazhkin and O. B. Tsiok, Phys. Rev. B **96**, 134111 (2017).
22. O. B. Tsiok and V. V. Brazhkin, J. Exp. Theor. Phys. **127**, 1118 (2018).

23. V. V. Brazhkin, E. Bychkov, and O. B. Tsiok, Phys. Chem. B **120**, 358 (2016).
24. V. V. Brazhkin, E. Bychkov, and O. B. Tsiok, J. Exp. Theor. Phys. **123**, 308 (2016).
25. V. V. Brazhkin, E. Bychkov, and O. B. Tsiok, J. Exp. Theor. Phys. **125**, 451 (2017).
26. L. G. Khvostantsev, V. N. Slesarev, and V. V. Brazhkin, High Press. Res. **24**, 371 (2004).
27. O. B. Tsiok, V. V. Bredikhin, V. A. Sidorov, and L. G. Khvostantsev, High Press. Res. **10**, 523 (1992).
28. O. B. Tsiok, V. V. Brazhkin, A. G. Lyapin, and L. G. Khvostantsev, Phys. Rev. Lett. **80**, 999 (1998).
29. V. V. Brazhkin, O. B. Tsiok, and Y. Katayama, JETP Lett. **89**, 244 (2009).
30. G. Lucovsky, Phys. Rev. B **6**, 1480 (1971).
31. M. Frumar, Z. Polák, and Z. Černošek, J. Non-Cryst. Solids **256–257**, 105 (1999).
32. T. L. Cottrell, *The Strengths of Chemical Bonds*, 2nd ed. (Butterworths, London, 1958).
33. L. Pauling, *The Nature of the Chemical Bond*, 3rd ed. (Cornell Univ. Press, Ithaca, 1960).
34. G. Williams and D. Watts, Trans. Faraday Soc. **66**, 80 (1970).
35. G. Z. Vinogradova, *Glass Formation and Phase Equilibria in Chalcogenide Systems* (Nauka, Moscow, 1984) [in Russian].
36. K. Richardson, T. Cardinal, M. Richardson, A. Schulte, and S. Seal, in *Photo-Induced Metastability in Amorphous Semiconductors*, Ed. by A. V. Kolobov (Wiley-VCH, Weinheim, 2003), p. 383.